

Multipeak dynamic magnetic susceptibility of a superparamagnetic nanoparticle suspended in a fluid

I. S. Poperechny ^{*}

*Institute of Continuous Media Mechanics, Russian Academy of Sciences, Ural Branch, Perm 614018, Russia
and Perm State National Research University, Perm 614068, Russia*

 (Received 6 January 2023; revised 30 January 2023; accepted 1 February 2023; published 13 February 2023)

Linear response theory for the case of a uniaxially anisotropic superparamagnetic nanoparticle suspended in a fluid is developed for the situations where, along with the probing field, a stationary bias field is present. The built up description allows for both mechanisms of magnetic relaxation available to the particle: the internal (relaxation of the magnetic moment inside the particle) and external (relaxation together with the particle body due to its Brownian orientation diffusion in a fluid). In this framework, longitudinal dynamic magnetic susceptibility of such a particle is considered. It is confirmed that at zero bias field, frequency dependence of the out-of-phase component of the dynamic susceptibility (absorption spectrum) has two maxima if anisotropy energy is only several times greater than thermal energy. The presence of these peaks is a direct consequence of the bistability of uniaxial magnetic nanoparticles. The magnetizing field changes position and height of these maxima. Moreover, it is shown that in a presence of the bias the spectrum can acquire a third maximum if the Brownian rotation of the suspended particle is retarded with respect to establishment of the intrinsic magnetic equilibrium in it. Necessary conditions for such a situation are analyzed, and criteria for the possible appearance of the additional third absorption peak are indicated.

DOI: [10.1103/PhysRevB.107.064416](https://doi.org/10.1103/PhysRevB.107.064416)

I. INTRODUCTION

The properties of magnetic particle ensembles dispersed in various media are a subject of intense studies for several decades. Despite that, the interest to these systems yet grows since the prospects of their application do not stop to extend. Just a very incomplete list of advanced trends comprises catalysis, spintronics, flexible [1] and organic [2] electronics, and diverse biomedical techniques [3–6].

An inherent property of magnetic nanoparticles is superparamagnetism—spontaneous remagnetizing—caused by thermal orientation fluctuations of the magnetic moment. To date, the magnetic response of mechanically fixed superparamagnetic nanoparticles has been well studied, see for example Ref. [7].

The theory of the magnetic response of nanoparticles suspended in a fluid is much less developed. This concerns even a seemingly nonsophisticated situation where the particles are uniaxial, i.e., possess the simplest type of magnetic anisotropy, and the exciting field is weak, so that the problem may be solved in the linear response approximation. The cornerstone of the modern theory of nanoparticle magnetodynamics in a fluid is a Fokker-Planck-type kinetic equation for the joint distribution function of two angle variables: the directions of the particle magnetic moment and its easy-magnetization axis. For the first time, this equation had been derived in Ref. [8] from semiphenomenological considerations in the framework of the so called “egg” model. Much

later, in Refs. [9] and [10] the appropriate stochastic Langevin equations for that model were formulated.

Finding a solution of the kinetic equation is a quite complicated task due to the multidimensionality of the configurational space one needs to deal with. An eligible method to handle the problem was outlined in Ref. [11]. Its main idea is to expand the sought-for distribution function over a full set of functions defined in the phase space of the system and then to transit to recurrence-differential relations for the functional expansion coefficients. In Ref. [11] as the basis for that expansion, a direct product of two sets of spherical harmonics has been chosen: one of them is defined with respect to the angle coordinates of the magnetic moment vector whereas the other is with respect to the angle coordinates of the anisotropy axis. This factorization enabled the authors to obtain numerically the frequency dependence of dynamic magnetic susceptibility of a superparamagnetic particle suspended in a fluid under zero constant field. Later on, in Ref. [12] simple and handy approximation formulas for this dependence were found. Another way to solve the kinetic equation was presented in Ref. [13]. Its essential distinction from that of Ref. [11] is the change of representation for the kinetic operator. Indeed, in Ref. [13] the basis for the functional space is built on the so-called bipolar harmonics which realize an irreducible tensor product of two spherical harmonics whose sets of arguments are different.

An alternative equation for the joint distribution function was proposed in Ref. [14]. Recently it was used in Ref. [15] to study magnetic response of a particle suspended in a fluid and subjected to a constant magnetizing field. By performing numerical calculations, authors of Ref. [15] inferred that

*ipoperchny@gmail.com

at any bias field dynamic magnetic susceptibility of such a particle could be described by a simple Debye-like formula. Moreover, it was stressed that qualitatively the same finding should follow from the kinetic equation derived in Ref. [8].

Nonetheless, very recent results of Ref. [16] do not correspond to this conclusion. Based on the “egg” model, the authors of Ref. [16] have analyzed both the relaxation spectrum and frequency dependences of the dynamic magnetic susceptibility of an ensemble of nanoparticles suspended in a fluid, and showed that absorption spectrum of such a system can possess two maxima, and therefore, in general case, it is not described by a single Lorentz-type function, as it was stated in Ref. [15].

In this paper, within the framework of Ref. [13], a theory of the linear response of superparamagnetic particles suspended in a fluid in the presence of a constant magnetizing field has been extended. The proposed description not only confirms results of Ref. [16] but also leads to another important conclusion: application of the bias field to a suspension of superparamagnetic nanoparticles may result in an additional, third low-frequency absorption peak.

II. SOLUTION OF THE KINETIC EQUATION

A. Kinetic equation (gyration-free approximation)

Consider a single-domain ferromagnetic (or ferrite) nanoparticle with magnetic moment $\boldsymbol{\mu}$ whose value at the given temperature is constant. It is assumed that the particle possesses uniaxial magnetic anisotropy with the energy density K and direction defined by a unit vector \mathbf{n} . As the easy-magnetization axis is fixed with respect to the particle body, vector \mathbf{n} may be taken as a marker indicating orientation of the particle as a mechanical object.

In a nanosuspension the direction of the particle magnetic moment—it is convenient to describe it by a unit vector $\mathbf{e} = \boldsymbol{\mu}/\mu$ —changes randomly due to two reasons. First, vector \mathbf{e} , as well as \mathbf{n} , rotate chaotically together with the particle under collisions with molecules of the fluid environment. Second, provided that thermal energy is comparable with the anisotropy one, vector \mathbf{e} deviates spontaneously from the easy axis, so that the angle between \mathbf{e} and \mathbf{n} is a fluctuating quantity.

In such a situation, a full account of the particle state is delivered by the joint distribution function $W(t, \mathbf{e}, \mathbf{n})$ that depends on the orientations of both reference unit vectors. This distribution function evolves according to a closed equation that has the form

$$\frac{\partial W}{\partial t} = \hat{S}W, \quad (1)$$

where \hat{S} is the operator that determines the behavior of the system out of equilibrium (kinetic operator). All the observable magnetic and orientation characteristics of an assembly of noninteracting particles at any given time instant can be found by averaging the respective phase variable with $W(t, \mathbf{e}, \mathbf{n})$.

In Refs. [8] and [13] it is shown that, provided the reference time of the magnetic field variation is far greater than the period of magnetic moment precession, the kinetic operator

may be presented in the gyration-free approximation as

$$\hat{S}W = \frac{1}{2\tau_B}(\hat{\mathbf{J}}_e + \hat{\mathbf{J}}_n) \cdot W(\hat{\mathbf{J}}_e + \hat{\mathbf{J}}_n) \left(\frac{U}{T} + \ln W \right) + \frac{1}{2\tau_D} \hat{\mathbf{J}}_e \cdot W \hat{\mathbf{J}}_e \left(\frac{U}{T} + \ln W \right), \quad (2)$$

where U is the orientation-dependent part of the magnetic energy of the particle, T is the temperature of the system, and vector operators $\hat{\mathbf{J}}_e$ and $\hat{\mathbf{J}}_n$ are defined as

$$\hat{\mathbf{J}}_e = \mathbf{e} \times \frac{\partial}{\partial \mathbf{e}}, \quad \hat{\mathbf{J}}_n = \mathbf{n} \times \frac{\partial}{\partial \mathbf{n}}. \quad (3)$$

Solution of equation $\hat{S}W_0 = 0$ renders the equilibrium distribution function of the system:

$$W_0(\mathbf{e}, \mathbf{n}) = \frac{1}{Z} \exp(-U/T), \quad Z = \int d\mathbf{n} \int d\mathbf{e} \exp(-U/T), \quad (4)$$

which means that the kernel of the kinetic operator has the Boltzmann form.

The times τ_B and τ_D in Eq. (2) are expressed in terms of the material parameters of the particle and its environment:

$$\tau_B = 3\eta V/T, \quad \tau_D = (1 + \alpha^2)\mu/2\alpha\gamma T, \quad (5)$$

where η is the dynamic viscosity of the fluid, V is the particle volume, α is the damping parameter of Larmor precession, and γ is the gyromagnetic ratio. Physically, τ_B defines the reference time of Brownian rotary diffusion of the particle body, whereas τ_D sets the time scale of the internal superparamagnetic relaxation of the magnetic moment (\mathbf{e} with respect to \mathbf{n}) for the case where thermal energy is far greater than the anisotropy one.

In the presence of external field \mathbf{H} , the particle energy U comprises the Zeeman and anisotropy contributions:

$$U = -\boldsymbol{\mu} \cdot \mathbf{H} - KV(\mathbf{e} \cdot \mathbf{n})^2. \quad (6)$$

In units of thermal energy, function Eq. (6) takes the form

$$\frac{U}{T} = -\xi(\mathbf{e} \cdot \mathbf{q}) - \sigma(\mathbf{e} \cdot \mathbf{n})^2, \quad (7)$$

where nondimensional parameters for the magnetic field strength and anisotropy energy are introduced as

$$\xi = \mu H/T, \quad \sigma = KV/T, \quad (8)$$

and $\mathbf{q} = \mathbf{H}/H$ is a unit vector in the direction of applied field.

B. Matrix form of the kinetic equation

To solve Eq. (1), the distribution function $W(t, \mathbf{e}, \mathbf{n})$ is expanded, following the scheme of Ref. [13], in a series of

bipolar harmonics $Y_{l_1 l_2}^{LM}$:

$$W(t, \mathbf{e}, \mathbf{n}) = \sum_{l_1=0}^{\infty} \sum_{l_2=0}^{\infty} \sum_{L'=|l_1-l_2|}^{l_1+l_2} \sum_{M'=-L'}^{L'} b_{l_1 l_2}^{L' M'}(t) Y_{l_1 l_2}^{L' M'}(\mathbf{e}, \mathbf{n}), \quad (9)$$

with the explicit expressions for the harmonics, see Ref. [17]:

$$Y_{l_1 l_2}^{LM}(\mathbf{e}, \mathbf{n}) = \sum_{m_1=-l_1}^{l_1} \sum_{m_2=-l_2}^{l_2} C_{l_1 m_1 l_2 m_2}^{LM} Y_{l_1 m_1}(\mathbf{e}) Y_{l_2 m_2}(\mathbf{n}), \quad m_2 = M - m_1, \quad (10)$$

where Y_{lm} , defined on a sphere of unit radius, are

$$Y_{lm}(\vartheta, \varphi) = (-1)^m \sqrt{\frac{(2l+1)(l-m)!}{4\pi(l+m)!}} P_{lm}(\cos \vartheta) e^{im\varphi}, \quad -l \leq m \leq l. \quad (11)$$

Here P_{lm} denotes the associated Legendre polynomials. The employed bipolar harmonics make a full set in the functional space whose elements depend on the angular coordinates of vectors \mathbf{e} and \mathbf{n} and are orthonormalized:

$$\begin{aligned} \langle Y_{l_1 l_2}^{LM} | Y_{l_1' l_2'}^{L' M'} \rangle &= \int d\mathbf{e} \int d\mathbf{n} (Y_{l_1 l_2}^{LM}(\mathbf{e}, \mathbf{n}))^* \cdot Y_{l_1' l_2'}^{L' M'}(\mathbf{e}, \mathbf{n}) = \delta_{l_1 l_1'} \delta_{l_2 l_2'} \delta_{LL'} \delta_{MM'}, \\ \int d\mathbf{e} &= \int_0^{2\pi} d\varphi_e \int_0^\pi d\vartheta_e \sin \vartheta_e, \quad \int d\mathbf{n} = \int_0^{2\pi} d\varphi_n \int_0^\pi d\vartheta_n \sin \vartheta_n. \end{aligned} \quad (12)$$

The specific advantage of functions $Y_{l_1 l_2}^{LM}$ is that they are eigenfunctions of the kinetic operator in situations where the magnetic energy is far lower than thermal one [13]:

$$\hat{S} Y_{l_1 l_2}^{LM} = -\lambda_{l_1 l_2}^{LM} \cdot Y_{l_1 l_2}^{LM}, \quad \lambda_{l_1 l_2}^{LM} = \frac{L(L+1)}{2\tau_B} + \frac{l_1(l_1+1)}{2\tau_D}, \quad \text{at } \frac{U}{T} \rightarrow 0. \quad (13)$$

In other words, in this limit the kinetic operator matrix is diagonal.

In a general case U/T is not constant and depends on the orientations of \mathbf{e} and \mathbf{n} , and the matrix of operator \hat{S} loses diagonality. The essential advantage of bipolar harmonic basis is that the resulting matrix comes out quite sparse. As it is shown in Ref. [13], under arbitrary ξ and σ the matrix elements of the kinetic operator are

$$\begin{aligned} \langle l_1, l_2, L, M | \hat{S} | l_1', l_2', L', M' \rangle &= \int d\mathbf{e} \int d\mathbf{n} (Y_{l_1 l_2}^{LM}(\mathbf{e}, \mathbf{n}))^* \cdot \hat{S} Y_{l_1' l_2'}^{L' M'}(\mathbf{e}, \mathbf{n}) \\ &= \frac{1}{2\tau_B} \left\{ -L(L+1) \cdot \delta_{l_1 l_1'} \delta_{l_2 l_2'} \delta_{LL'} \delta_{MM'} - \xi \frac{2\pi}{\sqrt{3}} [L'(L'+1) - L(L+1) - 2] B_{l_1' l_2' L' 101}^{l_1 l_2 L} \right\} \\ &\quad + \frac{1}{2\tau_D} \left\{ -l_1'(l_1'+1) \cdot \delta_{l_1 l_1'} \delta_{l_2 l_2'} \delta_{LL'} \delta_{MM'} - \xi \frac{2\pi}{\sqrt{3}} C_{L' M' 10}^{L M} [l_1'(l_1'+1) - l_1(l_1+1) - 2] B_{l_1' l_2' L' 101}^{l_1 l_2 L} \right. \\ &\quad \left. - \sigma \frac{4\pi}{\sqrt{45}} C_{L' M' 10}^{L M} [l_1'(l_1'+1) - l_1(l_1+1) - 6] B_{l_1' l_2' L' 220}^{l_1 l_2 L} \right\}. \end{aligned} \quad (14)$$

The coefficients of Eq. (14) expand as

$$B_{l_1' l_2' L' 101}^{l_1 l_2 L} = \frac{\sqrt{(2l_1'+1)(2l_2'+1)(2L'+1)(2l_1+1)(2l_2+1)(2L+1)}}{4\pi} C_{l_1' 0 l_1 0}^{l_1 0} C_{l_2' 0 l_2 0}^{l_2 0} \begin{Bmatrix} l_1' & l_1 & l_1' \\ l_2' & l_2 & l_2' \\ L' & L & L' \end{Bmatrix}, \quad (15)$$

where braces denote the Wigner 9j symbol [17].

Substituting series Eq. (9) in Eq. (1), one gets a set of linear equations for coefficients $b_{l_1 l_2}^{L' M'}(t)$:

$$\begin{aligned} \frac{db_{l_1 l_2}^{L' M'}(t)}{dt} &= \sum_{l_1'=0}^{\infty} \sum_{l_2'=0}^{\infty} \sum_{L'=|l_1'-l_2'|}^{l_1'+l_2'} \sum_{M'=-L'}^{L'} \\ &\quad \times \langle l_1, l_2, L, M | \hat{S} | l_1', l_2', L', M' \rangle b_{l_1' l_2'}^{L' M'}(t), \end{aligned} \quad (16)$$

which is nonuniform as its right-hand part includes the terms proportional to time-independent coefficient $b_{00}^{00} = 1/4\pi$. By introducing a column vector \mathbf{X} whose components consist of the ordered in a certain way coefficients $b_{l_1 l_2}^{L' M'}(t)$, one casts the

set of equations in Eq. (16) in a compact matrix form:

$$2\tau_D \frac{d\mathbf{X}}{dt} = \hat{\mathbf{A}}\mathbf{X} + \mathbf{B}. \quad (17)$$

The ordering of coefficients is performed as follows. Each element of vector \mathbf{X} is associated with four numbers ('multiindex') in such a way that $\mathbf{X}[l_1, l_2, L, M] = b_{l_1 l_2}^{L M}$. The elements of matrix $\hat{\mathbf{A}}$ are obtained by multiplying Eq. (14) by $2\tau_D$ whereas the numbers constituting column vector \mathbf{B} are proportional to b_{00}^{00} . After these rearrangements, numerical integration of the set in Eq. (17) may be carried out by any conventional method.

C. High-anisotropy approximation

Provided the anisotropy energy is much higher than thermal energy $\sigma = KV/T \gg 1$, one may neglect the non-collinearity of vectors \mathbf{e} and \mathbf{n} , and use the so-called ‘rigid-dipole’ approximation. In this limit, the magnetic energy in Eq. (7) reduces to $U/T = -\xi(\mathbf{n} \cdot \mathbf{h})$, and the distribution function depends only on the angle coordinates of vector \mathbf{n} and time, $W = W(t, \mathbf{n})$. As a result, the kinetic operator simplifies:

$$\hat{S}W = \frac{1}{2\tau_B} \hat{\mathbf{J}}_n \cdot W \hat{\mathbf{J}}_n \left(\frac{U}{T} + \ln W \right), \quad (18)$$

$$\langle l, m | \hat{S} | l', m' \rangle = \int d\mathbf{n} Y_{l,m}^* \cdot \hat{S} Y_{l',m'} = \frac{1}{2\tau_B} \left\{ -\xi \sqrt{\frac{l'^2 - m'^2}{4l'^2 - 1}} (l' - 1) \delta_{l',-1,l} \cdot \delta_{m',m} + \xi \sqrt{\frac{((l'+1)^2 - m'^2)}{4(l'+1)^2 - 1}} (l' + 2) \delta_{l'+1,l} \cdot \delta_{m',m} - l'(l'+1) \delta_{ll'} \cdot \delta_{mm'} \right\}. \quad (21)$$

To arrange this set to the same form Eq. (17), as in the aforementioned case of finite σ 's, it suffices to introduce a column vector \mathbf{X} with components b_{lm} and include in vector \mathbf{B} all the terms proportional to $b_{00} = 1/\sqrt{4\pi}$.

III. LINEAR APPROXIMATION AND LONGITUDINAL DYNAMIC SUSCEPTIBILITY

In general, the developed approach enables one to evaluate the magnetic response of a superparamagnetic particle suspended in a fluid for any time dependence of external field. Hereby the case where the system is subjected to a combination of a stationary bias field \mathbf{H}_0 and low-amplitude linearly polarized AC field, $\mathbf{h}(t)$ is considered. It is assumed that those fields are collinear, so that the net nondimensional field acting on a particle is $\xi_0 + \xi(t)$, with $\xi_0 = \mu H_0/T$ and $\xi(t) = \mu h(t)/T$. Given that, matrix \hat{A} and column vector \mathbf{B} of Eq. (17) are presented as

$$\hat{A} = \hat{A}_0 + \xi(t) \hat{A}_1, \quad \mathbf{B} = \mathbf{B}_0 + \xi(t) \mathbf{B}_1, \\ \hat{A}_0 = \hat{A}(\xi_0), \quad \mathbf{B}_0 = \mathbf{B}(\xi_0),$$

and the solution is constructed as a sum of a stationary equilibrium and a time-dependent perturbed parts:

$$\mathbf{X} = \mathbf{X}_0 + \mathbf{X}_1. \quad (22)$$

Assuming that the probing field is weak ($\xi(t) \ll 1$), vector $\mathbf{X}(t)$ may be evaluated in the first order in $\xi(t)$. The equilibrium contribution \mathbf{X}_0 is, evidently, determined from the zero-order equation

$$\hat{A}_0 \mathbf{X}_0 + \mathbf{B}_0 = 0,$$

whereas the nonequilibrium part is obtained from equation

$$2\tau_D \frac{d\mathbf{X}_1}{dt} = \hat{A}_0 \mathbf{X}_1 + \xi(t) (\hat{A}_1 \mathbf{X}_0 + \mathbf{B}_1). \quad (23)$$

so that appropriate basis may be constructed of plain spherical harmonics Y_{lm} , and the distribution function expands as

$$W(t, \mathbf{n}) = \sum_{l'=0}^{\infty} \sum_{m'=-l'}^{l'} b_{l'm'}(t) Y_{l'm'}(\mathbf{n}). \quad (19)$$

Upon substituting this expression in the kinetic equation, one arrives at the set

$$\frac{db_{lm}}{dt} = \sum_{l'=0}^{\infty} \sum_{m'=-l}^l \langle l, m | \hat{S} | l', m' \rangle b_{l'm'}(t), \quad (20)$$

where the operator matrix elements are

By performing Fourier transformation over time, one can transform Eq. (23) to the algebraic form:

$$(2i\omega\tau_D \hat{I} - \hat{A}_0) \mathbf{X}_1^\omega = (\hat{A}_1 \mathbf{X}_0 + \mathbf{B}_1) \xi_\omega. \quad (24)$$

Here \hat{I} is a unit matrix whereas ξ_ω and \mathbf{X}_1^ω are the Fourier transforms of the perturbation and response, respectively. Therefore, in the frequency domain the nonequilibrium part of the solution of the kinetic equation is

$$\mathbf{X}_1^\omega = \mathbf{R}_\omega \cdot \xi_\omega, \quad (25)$$

where

$$\mathbf{R}_\omega = (2i\omega\tau_D \hat{I} - \hat{A}_0)^{-1} \cdot (\hat{A}_1 \mathbf{X}_0 + \mathbf{B}_1). \quad (26)$$

The resulting solution enables one to find the dynamic magnetic susceptibility of the suspended nanoparticle. Denoting the angle between vectors \mathbf{e} and \mathbf{H}_0 as ϑ_e , the expression for the average projection of the system magnetization on the direction of \mathbf{H}_0 comes out as

$$M(t) = \frac{\mu}{V} \langle \cos \vartheta_e \rangle = \frac{4\pi}{\sqrt{3}} \frac{\mu}{V} \langle Y_{10}^{10} \rangle = \frac{4\pi}{\sqrt{3}} \frac{\mu}{V} \langle W | Y_{10}^{10} \rangle \\ = \frac{4\pi}{\sqrt{3}} \frac{\mu}{V} \cdot b_{10}^{10}(t) = \frac{4\pi}{\sqrt{3}} \frac{\mu}{V} \cdot \mathbf{X}(t) \\ [l_1 = 1, l_2 = 0, L = 1, M = 0]. \quad (27)$$

Here it is taken into account that scalar product $\langle W | Y_{10} \rangle$ equals $b_{l_1 l_2}^{LM}(t)$ due to orthonormality of bipolar harmonics.

Using vector of state in Eq. (22) to evaluate magnetization $M(t)$, the Fourier transform of the latter may be cast as

$$M_\omega = \chi(\omega) h_\omega, \quad (28)$$

so that explicit form of the linear dynamic susceptibility is

$$\chi(\omega) = \frac{4\pi}{\sqrt{3}} \cdot \frac{\mu^2}{VT} \cdot \mathbf{R}_\omega [l_1 = 1, l_2 = 0, L = 1, M = 0]. \quad (29)$$

In what follows, in order to facilitate tracing of the frequency and bias-field dependences, instead of full χ rendered by

Eq. (29) its normalized form is used:

$$\tilde{\chi}(\omega) = \tilde{\chi}'(\omega) - i\tilde{\chi}''(\omega) = \frac{4\pi}{\sqrt{3}} \cdot \mathbf{R}_\omega$$

$$[l_1 = 1, l_2 = 0, L = 1, M = 0]. \quad (30)$$

In the rigid-dipole limit ($\sigma \gg 1$), vector \mathbf{R}_ω is also determined by Eq. (26) but the matrix elements are calculated not via general formula [Eq. (14)] but with the aid of the simplified one, viz., Eq. (21). The corresponding susceptibility is

$$\chi(\omega) = \sqrt{\frac{4\pi}{3}} \frac{\mu^2}{VT} \mathbf{R}_\omega [l = 1, m = 0], \quad (31)$$

or, in the normalized form,

$$\tilde{\chi}(\omega) = \sqrt{\frac{4\pi}{3}} \mathbf{R}_\omega [l = 1, m = 0]. \quad (32)$$

The dynamic magnetic susceptibility of a superparamagnetic nanoparticle suspended in a fluid depends on the ratio $\zeta = \tau_D/\tau_B$, which is inversely proportional to the dynamic viscosity η . A simple estimate of possible values of the parameter ζ was made in Ref. [11]. For typical ferrite particles dispersed in water (the dynamic viscosity is about $\eta \sim 0.01$ P), the parameter is $\zeta \sim 10^{-2} - 10^{-3}$; if the medium is glycerin with viscosity $\eta \sim 10$ P, then the value decreases to $\zeta \sim 10^{-5} - 10^{-6}$.

The results of numerical evaluation of the normalized function $\tilde{\chi}(\omega)$ for viscosity parameter $\zeta = 10^{-3}$ in the case of zero bias field are presented in Fig. 1; different curves correspond to different values of the anisotropy parameter σ . As it is seen, at $H_0 = 0$ the imaginary part of the susceptibility $\tilde{\chi}''(\omega)$ in a general case possesses not one, but two maxima, to which correspond sharp depressions at the plots of the real (in-phase) part $\tilde{\chi}'(\omega)$.

The low-frequency ($\omega\tau_D < 1$) regions of the curves in Fig. 1 are well described by equations

$$\chi(\omega) = \frac{\mu^2}{3VT} \cdot \left[\frac{B(\sigma)}{1 + i\omega\tau} + 1 - B(\sigma) \right],$$

$$\tilde{\chi}(\omega) = \frac{1}{3} \cdot \left[\frac{B(\sigma)}{1 + i\omega\tau} + 1 - B(\sigma) \right], \quad (33)$$

proposed in Ref. [12]. Here function $B(\sigma)$ increases monotonically from $1/3$ to 1 while the anisotropy parameter σ grows from 0 to ∞ , and effective relaxation time is defined as

$$\tau = \frac{\tau_N \tau_B}{\tau_N + \tau_B}, \quad (34)$$

where τ_N could be found using the interpolation expression [18]

$$\tau_N = \tau_D \cdot \frac{e^\sigma - 1}{2\sigma} \left[\frac{1}{1 + 1/\sigma} \sqrt{\frac{\sigma}{\pi}} + 2^{-\sigma-1} \right]^{-1}. \quad (35)$$

Thus, at zero bias field, inside the interval $\omega\tau_D < 1$ the magnetic response of the system can be considered as a result of the joint rotary diffusion of the particle body (reference time τ_B) and internal Néel relaxation (reference time τ_N). As Fig. 1 shows, under the increase of the anisotropy parameter σ the low-frequency peak shifts leftward. This is an evident consequence of the fact that the growth of σ entails augmentation of

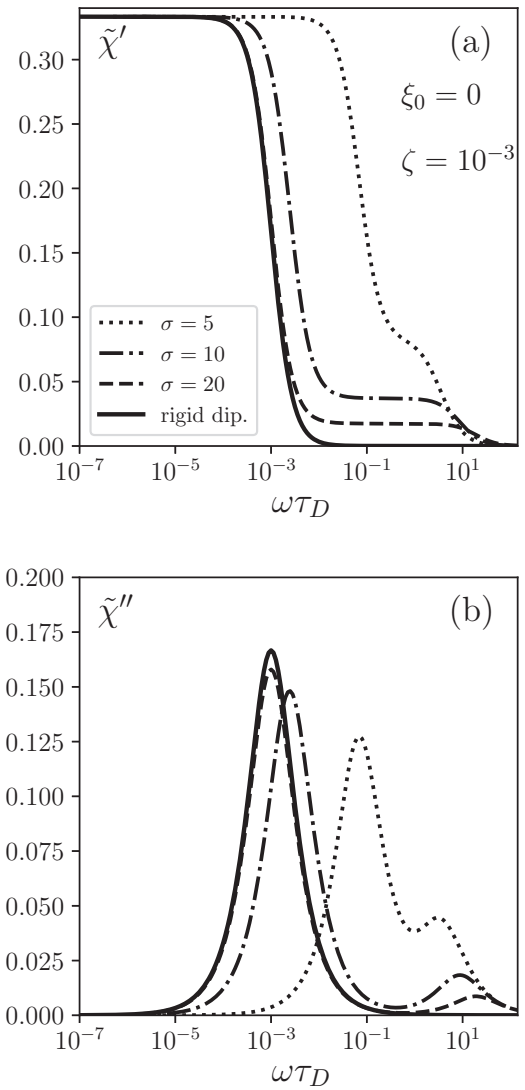


FIG. 1. Frequency dependences of real (a) and imaginary (b) components of the dynamic magnetic susceptibility in zero bias field ($\xi_0 = 0$) for different values of anisotropy parameter σ : 5 (dots), 10 (dot-dashes), 20 (dashes). Solid lines render the predictions of the rigid-dipole model. Parameter $\zeta = 10^{-3}$.

τ_N and, thus, the enhancement of the total time τ of magnetic relaxation of the particle. In $\sigma \rightarrow \infty$ limit, the Néel relaxation ‘freezes’ ($\tau_N \rightarrow \infty$), and the peak sets at $\omega = 1/\tau_B$, so that $\omega\tau_D = \zeta$ for it. The curves for that case are plotted in Fig. 1 by solid lines.

The second maximum of the frequency dependence of $\tilde{\chi}''$ (absorption spectrum) is located in the range $\omega\tau_D \gtrsim 1$ where formulas in Eq. (33) are no longer valid. As seen from Fig. 1, in this range the magnetic response also depends on the anisotropy parameter: both components of the dynamic susceptibility fall down with σ growth and tend to zero as $\sigma \rightarrow \infty$. Thus, one can conclude that in this range the magnetic response is solely controlled by internal (superparamagnetic) diffusion of the magnetic moment: the limit $\sigma \rightarrow \infty$ implies its total cessation. It should be noted that the high-frequency peak in Fig. 1 is not related to ferromagnetic resonance since in the adopted gyration-free approximation

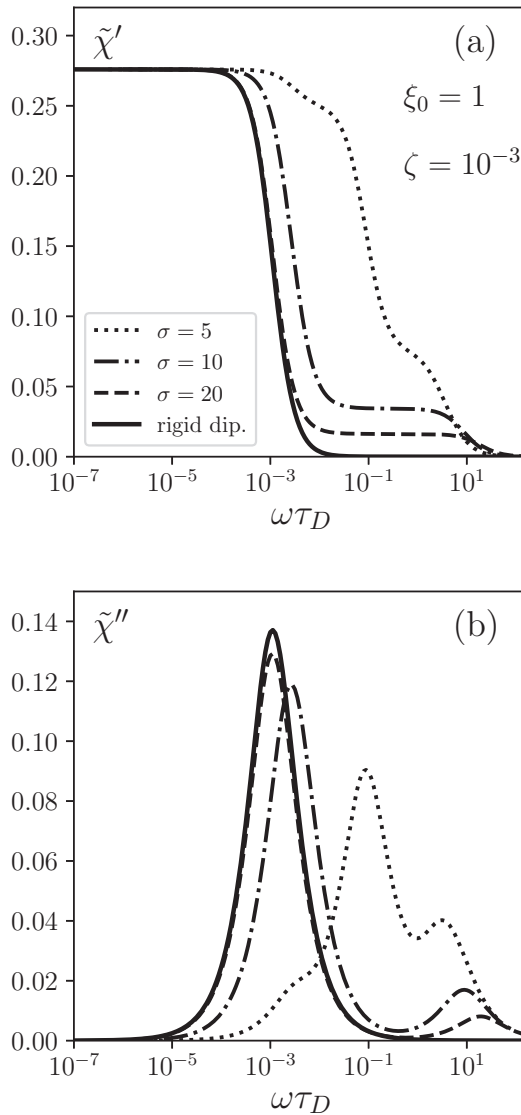


FIG. 2. Frequency dependences of real (a) and imaginary (b) components of the dynamic magnetic susceptibility under a moderate bias field ($\xi_0 = 1$) for different values of anisotropy parameter σ : 5 (dots), 10 (dot-dashes), 20 (dashes). Solid lines render the predictions of the rigid-dipole model. Parameter $\zeta = 10^{-3}$.

the system does not at all have eigenfrequencies (all eigenvalues of the kinetic operator are real). The abrupt growth of susceptibility $\tilde{\chi}''(\omega)$ at $\omega\tau_D \sim 1$ merely indicates the presence of relaxation modes with reference times $\sim \tau_D$ in the particle spectrum. Those are the processes of intrawell kind: stochastic wandering of the magnetic moment in the vicinities of the energy minima [19]. As to the resonance properties of nanosuspensions of anisotropic superparamagnetic particles, some relevant results one can find in Refs. [20] and [21].

In Figs. 2 and 3 frequency dependences of the dynamic susceptibility components are shown under finite bias fields. In the first case (Fig. 2), the Zeeman energy of the particles equals to thermal energy ($\xi_0 = 1$) whereas in the second case (Fig. 3) the magnetic energy is ten times greater ($\xi_0 = 10$). Comparison of the curves evidences that application of a stationary bias field reduces the magnetic response. Indeed,

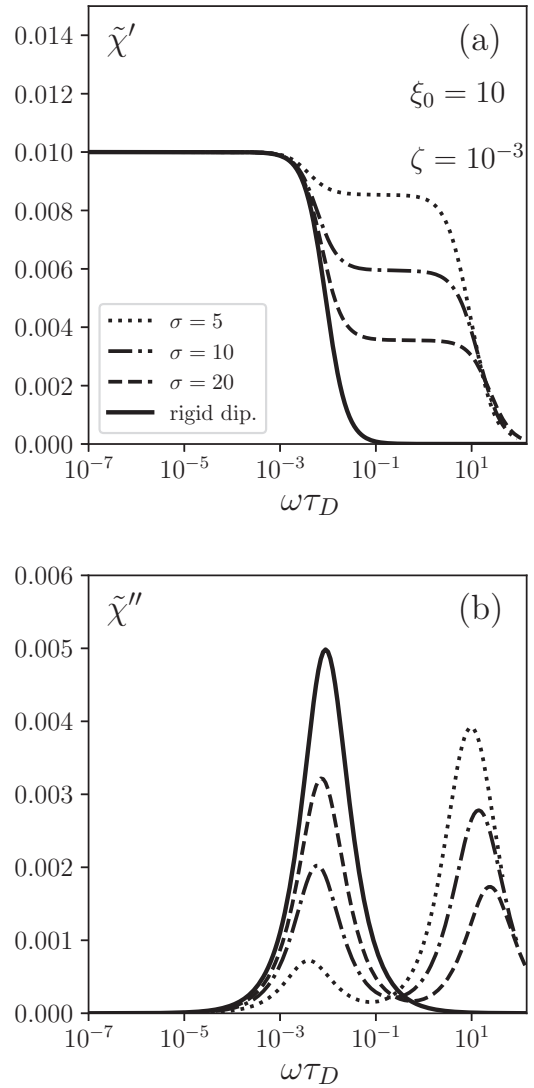


FIG. 3. Frequency dependences of real (a) and imaginary (b) components of the dynamic magnetic susceptibility under a strong bias field ($\xi_0 = 10$) for different values of anisotropy parameter σ : 5 (dots), 10 (dot-dashes), 20 (dashes). Solid lines render the predictions of rigid-dipole model. Parameter $\zeta = 10^{-3}$.

a perturbation of the magnetic state of a particle on the part of probing field is the more significant the greater the angle between vectors \mathbf{n} and \mathbf{h} . Meanwhile, application of a bias field induces orientation ordering of the particles: their easy axes by and large align with the direction of \mathbf{H}_0 , and due to that the angle between \mathbf{n} and \mathbf{h} goes down on the average. Besides that, the magnetic relaxation times decrease as the bias field strength grows, and this induces a certain shift of the dispersion regions of both $\chi'(\omega)$ and $\chi''(\omega)$ to higher frequencies. The seeming exception is dotted curves that correspond to $\sigma = 5$: the left peak at $\xi_0 = 10$ (Fig. 3) is located to the right of that at $\xi_0 = 0$ (Fig. 1). The reasons for such an effect are discussed below.

Remarkably, as Fig. 2(b) shows, at certain values of the anisotropy parameter σ the bias field might give birth to an additional, third peak of the absorption line. This is indicated

by dotted curve for $\sigma = 5$: its inflection at $\omega\tau_D \sim 5 \cdot 10^{-3}$ is quite clear.

IV. DISCUSSION

In the case of zero bias field the presence of two peaks on the absorption spectrum is a direct consequence of the bistability of a uniaxial magnetic nanoparticle: its energy profile has two minima separated by a potential barrier if an applied field does not exceed a critical value $2KV/\mu \cdot (\sin^{2/3}\psi + \cos^{2/3}\psi)^{-3/2}$, where ψ is the angle between easy magnetization axis and the field direction. This fact enables one to divide the magnetic relaxation processes in a mechanically fixed uniaxial nanoparticle in two qualitatively different families [19,22,23]. The first one comprises a countable number of the already mentioned intrawell modes which are due to thermal motion of the magnetic moment around the energy minima and cause an absorption maximum of relaxation origin at $\omega\tau_D \sim 1$. The second set consists of a single (Néel, interwell) mode which originates from random transitions of the magnetic moment over the energy barrier. The respective relaxation time grows exponentially with the barrier height and yet at $\sigma \sim 5$ exceeds the reference time scale of the intrawell processes by an order of magnitude. Brownian motion of the particle body in a fluid evidently entails the overall changes of the relaxation spectrum in comparison with the case of a solid matrix, this may be seen from Eq. (34). However, the essential feature holds: the difference between the reference times still counts more than order of magnitude for $\sigma \gtrsim 5$. The direct consequence of the large distinction between the basic relaxation times are the two well-resolved peaks on the absorption line.

If the anisotropy energy does not exceed the thermal energy $\sigma \lesssim 1$, the differences between inter- and intrawell modes are erased: all reference relaxation times of an immobilized particle are $\sim\tau_D$ in this case (for example, $\tau_N = 1.5 \cdot \tau_D$ for $\sigma = 1$). In accordance with Eq. (34), this means that without the magnetizing field any reference time of the joint rotational diffusion of the particle body and its magnetic moment is close to τ_D provided $\sigma \lesssim 1$. In this situation the dynamic magnetic susceptibility of the particle follows a simple Debye expression $\tilde{\chi}(\omega) \approx 1/3 \cdot (1 + i\omega\tau_D)^{-1}$ (for $\sigma = 0$ this equality is exact). Thus, its out-of-phase part has the only maximum at the frequency $\omega\tau_D \approx 1$. Height of this maximum as well as the corresponding value of the in-phase component are approximately equal to half of the static susceptibility. This is demonstrated by dotted lines in Fig. 4, where frequency dependences of the functions $\tilde{\chi}'(\omega)$ and $\tilde{\chi}''(\omega)$ are shown for $\sigma = 1$ and $\zeta = 10^{-3}$.

Application of the bias field may, however, lead to appearance of an additional low-frequency absorption peak, see solid lines in Fig. 4(b). It is obviously impossible to explain this maximum only by the magnetic bistability of a uniaxial nanoparticle because at $\sigma = 1$ it does not play any role. This implies that the additional peak is inherently related to the Brownian rotation of the particle. Indeed, for $\sigma = 1$ a magnetic equilibrium state inside the particle is established over a time $\sim\tau_D$. Therefore, the absorption peak in the frequency range $\omega\tau_D \ll 1$ corresponds to the rotational diffusion of the body of the particle, whose intrinsic (with respect to

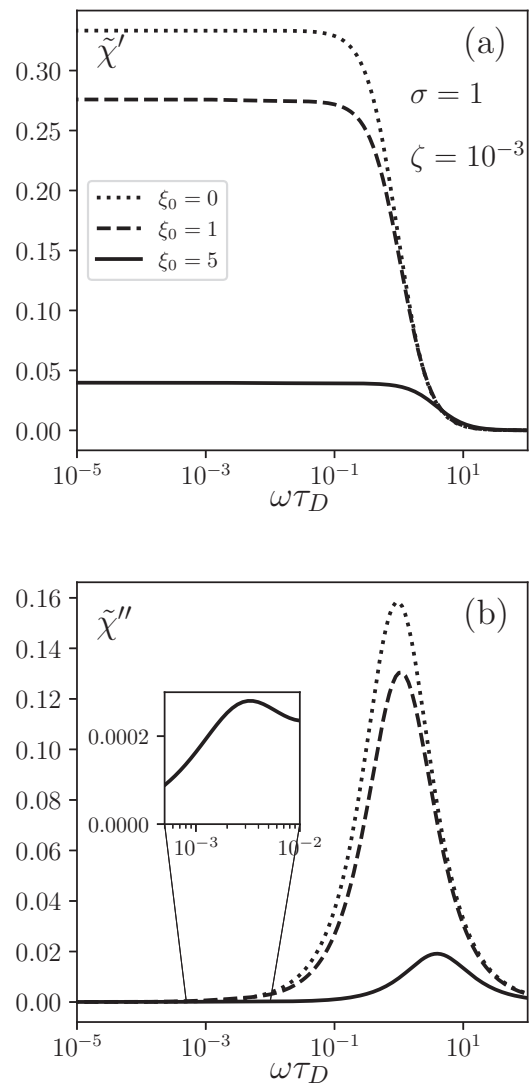


FIG. 4. Frequency dependences of real (a) and imaginary (b) components of the dynamic magnetic susceptibility under anisotropy parameter $\sigma = 1$ for different bias field magnitudes: $\xi_0 = 0$ (dots), 1 (dashes), 5 (solid lines); parameter $\zeta = 10^{-3}$. The inset shows the line for $\xi_0 = 5$ in the frequency range from $\omega\tau_D = 5 \cdot 10^{-4}$ to 10^{-2} .

anisotropy axis) magnetic relaxation is accomplished. The reference time for this case can be estimated using Eq. (13). In this formula values $l_1 = l_2 = L = 0$ correspond to statistical equilibrium of the system: the appropriate eigenvalue of the kinetic operator is equal to zero (the equilibrium distribution function is its kernel). The state of partial equilibrium, when the internal diffusion of the particle's magnetic moment is completed, but the diffusion of the body is not, is characterized by the values $l_1 = 0, L = l_2 \neq 0$. Since the anisotropy energy for a uniaxial particle does not change by substitution $\mathbf{n} \rightarrow -\mathbf{n}$, the smallest nonzero value l_2 should be chosen equal to two. Then it follows from Eq. (13) that the low-frequency peak on the solid line in Fig. 4(b) corresponds to a process when the reference value of inverse relaxation time is equal to $\lambda \cdot \tau_D = 3\tau_D/\tau_B = 3\zeta$. The position of the

low-frequency maximum near the point $\omega\tau_D = 3\zeta$ in the inset in Fig. 4 confirms this result.

Similarly, the presence of the third peak in Fig. 2 cannot be attributed to just magnetic bistability of the particle. Otherwise, it would have revealed itself in mechanically fixed nanoparticles as well. Meanwhile, as already mentioned, far below the ferromagnetic resonance range, the magnetic response of quiescent superparamagnetic nanoparticles is determined solely by the Néel mode, which produces just a single peak on the absorption line. From the numerical analysis it follows that the third maximum turns up if the anisotropy is not too high; for example, Fig. 2 shows that for viscosity parameter $\zeta = 10^{-3}$ it is present at $\sigma = 5$ but is absent at $\sigma = 10$. Given that, one may encounter a situation where the thermofluctuation interwell hopping rate is yet so high that the magnetic equilibrium inside the particle settles before the rotary diffusion of its body is accomplished.

Thus, the additional peak appears in the case when the Brownian relaxation of a suspended particle is retarded with respect to establishment of the intrinsic magnetic equilibrium in it. Note that this peak of absorption may occur only for the particle with nonzero equilibrium magnetic moment, that it exists only in the presence of a constant bias field. An increase of this field should lead to a better distinguishability of the third additional maximum. Indeed, the Néel relaxation time goes down exponentially as the applied field increases [24,25]. However, the dependence of the Brownian relaxation time on external field of even a particle whose magnetic moment is “frozen” into the body is much more weak ($\sim 1/\xi_0$), see Refs. [26–28]. In a situation where magnetic moment of the particle is not coaligned with anisotropy axis, but distributed according to Boltzmann function, one should expect an even smaller effect of the field because orientation thermal fluctuations of the magnetic moment effectively demagnetize the particle. Actually, according to Ref. [16], the smallest eigenvalue of the kinetic operator is almost independent on the bias field and $\approx 3/\tau_B$ in a wide range of values of the parameter ξ . Thus, a growth of the magnetizing field should lead to a relatively fast shift of the central (“Néel–Brownian”) absorption maximum to the right—to higher frequencies, but almost not change position of the left (“Brownian”) one. As a consequence, the frequency interval between the two peaks increases, and their resolution improves. The results of numerical calculations are in agreement with this reasoning, see Fig. 5, where absorption lines of the particle with parameters $\sigma = 5$ and $\zeta = 10^{-3}$ are shown for bias fields $\xi_0 > 1$; the corresponding curve for $\xi_0 = 1$ is plotted by dots in Fig. 2.

Nevertheless, Fig. 3 shows that if the Zeeman energy significantly exceeds the thermal one, then the absorption line has no more than two maxima, as in the case of a zero bias field. This is due to the fact that position of the high-frequency absorption maximum, as well as of the “Brownian” one, relatively weakly depends on the magnitude of the bias field. Therefore, as ξ_0 increases, the central peak moves away from the left (low-frequency) maximum, but approaches the right (high-frequency) one and eventually merges with it. According to Fig. 5, in the case of $\sigma = 5$ and $\zeta = 10^{-3}$ they cannot be resolved already at $\xi_0 \gtrsim 4$.

These considerations clarify why the left maximum on the dotted curve for $\sigma = 5$ in Fig. 3 (the bias field $\xi_0 = 10$) is

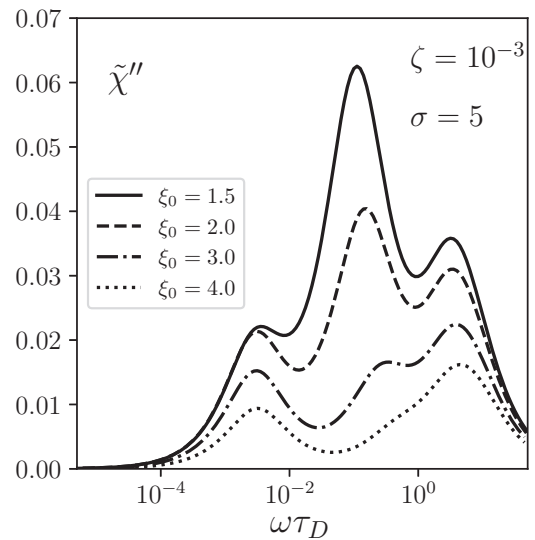


FIG. 5. Absorption spectra of a particle with $\sigma = 5$ for different values of bias field: $\xi_0 = 1.5$ (solid lines), 2 (dashes), 3 (dot-dashes), 4 (dots); parameter $\zeta = 10^{-3}$.

in the region of lower frequencies than the one in Fig. 1 (no bias field). At first glance, from this fact one could conclude that the relaxation time of the particle paradoxically decreases with the growth of the applied field. But in fact, the low-frequency maxima in these figures correspond to essentially different diffusion processes. At $\xi_0 = 0$, the left peak characterizes the joint Néel–Brownian relaxation: nonequilibrium transitions of the magnetic moment over the potential barrier together with the rotation of the particle body. However, for $\xi = 10$ it corresponds to rotational diffusion (in a magnetizing field) of a particle, whose intrinsic magnetic state is equilibrium. So, the relative position of the low-frequency maximum in the zero and strong bias field in this case does not mean at all that an increase in the external field slows down magnetic relaxation.

The time of intrinsic (interwell) relaxation of a particle grows exponentially with the increase of the anisotropy parameter σ at any angle between the anisotropy axis and direction of the applied field [7,24]. For sufficiently large σ , the necessary condition for the appearance of the third peak—relatively fast establishment of magnetic equilibrium inside the particle—may be unachievable. In this case, the two low-frequency peaks are not resolved. This situation is illustrated by Fig. 6(a), where absorption lines are shown for a system with the viscosity parameter $\zeta = 10^{-4}$ and the bias field $\xi_0 = 3$. As can be seen, the growth of σ leads to the convergence of two maxima, and at $\sigma_* \approx 11.5$ they merge. The value of σ_* , in general, depends on the magnitude of the magnetizing field. For $\xi_0 < 3$ it will be less than the specified one; however, an enhancement of the bias above $\xi_0 = 3$ almost does not change σ_* , mainly due to the rapid decrease in the height of the central peak with the field growth, compare Figs. 6(a) and 6(b) that differ only in the value of ξ_0 . Numerical analysis shows that for other values of ζ it is also enough to choose $\xi_0 = 3$ for estimation of σ_* .

It can be seen in Fig. 7 that the value of σ_* increases with the growth of dynamic viscosity η of a fluid, in which the

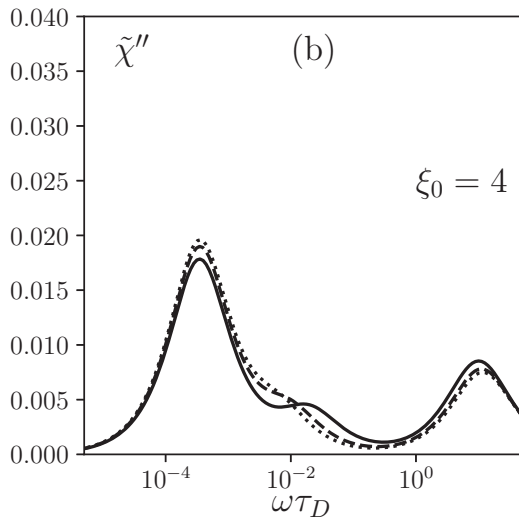
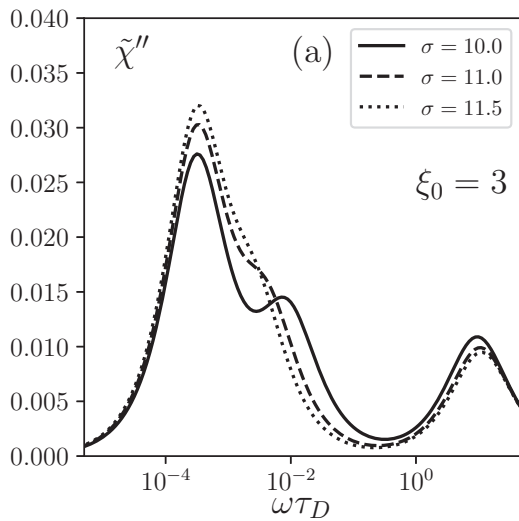


FIG. 6. Absorption spectra under bias field $\xi_0 = 3$ (a) and $\xi_0 = 4$ (b) for different values of anisotropy parameter: $\sigma = 10$ (solid lines), 11 (dashes), 11.5 (dots); parameter $\zeta = 10^{-4}$.

particle is suspended. This result is quite clear because the ratio between internal (Néel) and Brownian relaxation times is proportional to $\zeta \exp(\sigma) \propto \eta^{-1} \exp(\sigma)$. Therefore, the larger the viscosity of the fluid (the smaller the ζ parameter), the wider the range of values of σ , for which the Néel time is less than $\sim \tau_B/3$, the time that determines the position of the low-frequency “Brownian” peak. For the same reason, the dependence of σ_* on the parameter ζ is predominantly logarithmic, draw attention to logarithmic scale on the horizontal axis in Fig. 7. The absence of strict linearity is due to the fact that the pre-exponential factor in the expression for the Néel relaxation time also depends on σ . Note that the third maximum on the absorption line is possible even at $\zeta = 10^{-2}$, i.e., relatively low viscosity of the carrier fluid, if $\sigma \lesssim 5.5$. Results of numerical calculations in Fig. 8 illustrate this situation.

At last, point out that the lowest magnitude of the bias field, at which the absorption spectrum is three-peak, decreases as the viscosity parameter ζ goes down. For example, Fig. 9

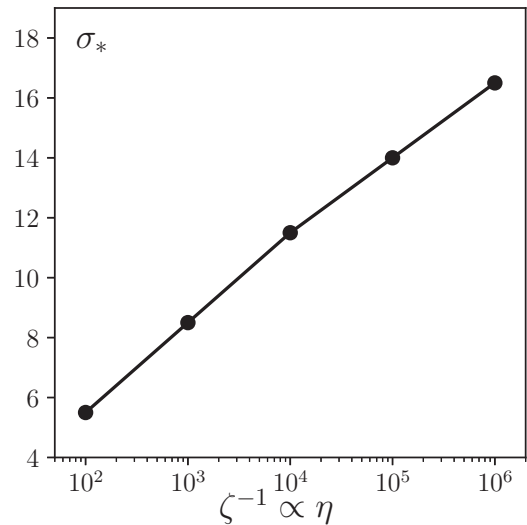


FIG. 7. Dependence of the upper limit σ_* of anisotropy parameter values, at which three-peak absorption spectrum is possible, on $\zeta^{-1} \propto \eta$, where η is the dynamic viscosity of a fluid.

shows that for $\zeta = 10^{-4}$ and $\sigma = 5$ the additional maximum is already distinct at $\xi_0 = 0.5$; for $\zeta = 10^{-3}$ and $\zeta = 10^{-2}$ this threshold is $\xi_0 \approx 1$ and $\xi_0 \approx 2$ correspondingly, see Figs. 2 and 8.

V. CONCLUSION

A consistent theory of linear magnetic response of a uniaxial single-domain nanoparticle suspended in a fluid is developed. The theory is based on the kinetic equation that takes into account the orientation diffusionlike motion of both the particle magnetic moment and its anisotropy axis. Under appropriate mathematical treatment, the multi-variable kinetic equation may be transformed to an infinite set of

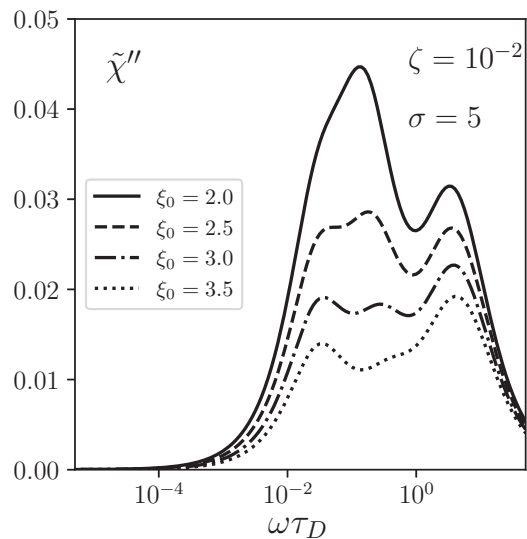


FIG. 8. Absorption spectra of a particle with $\sigma = 5$ for different values of bias field: $\xi_0 = 2$ (solid lines), 2.5 (dashes), 3 (dot-dashes), 3.5 (dots); parameter $\zeta = 10^{-2}$.

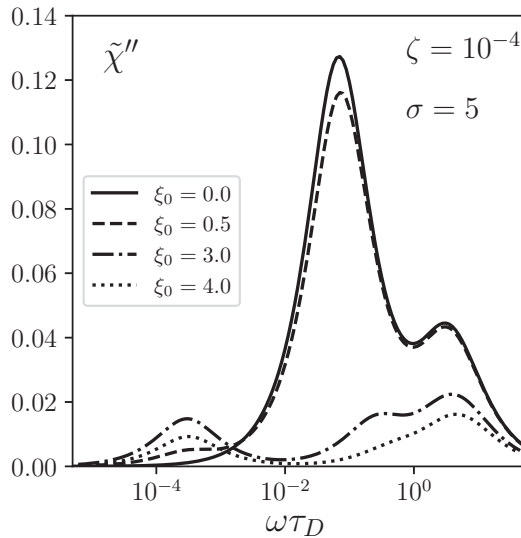


FIG. 9. Absorption spectra of a particle with $\sigma = 5$ for different values of bias field: $\xi_0 = 0$ (solid lines), 0.5 (dashes), 3 (dot-dashes), 4 (dots); parameter $\zeta = 10^{-4}$.

differential-recurrence equations of first order for the statistical moments of the pertinent distribution function. Upon

solving this set, the frequency dependences of the components of linear magnetic susceptibility of a superparamagnetic particle suspended in a fluid are evaluated for the situations where the system, along with a weak probing field, is subjected to a stationary bias field of arbitrary strength. It is shown that the imaginary (out-of-phase) component of the dynamic susceptibility—it defines the intensity of energy absorption—at a pronounced particle anisotropy should have two well-separated maxima. The heights and positions of these maxima are affected by the bias field. Also, in the presence of the magnetizing field the spectrum may acquire a third peak if the ratio between anisotropy energy and thermal one does not exceed some threshold, which grows mostly logarithmically with increasing fluid viscosity. The presented theoretical model does not impose any special restrictions on the material parameters of nanoparticles, viscosity of the suspending fluid and temperature, and may be used, in particular, for establishing validity ranges of various approximations.

ACKNOWLEDGMENTS

The work was supported by Russian Science Foundation under Grant No. 22-22-00288. The author is grateful to Prof. Yu. L. Raikher for fruitful discussions.

- [1] S. Khanra, A.-A. Mamun, F. F. Ferreira, K. Ghosh, and S. Guha, *ACS Appl. Nano Mater.* **1**, 1175 (2018).
- [2] Z. He, Z. Zhang, and S. Bi, *Mater. Res. Express* **7**, 012004 (2020).
- [3] S. Amiri and H. Shokrollahi, *Mater. Sci. Eng. Ser. C* **33**, 1 (2013).
- [4] S. Y. Srinivasan, K. M. Paknikar, D. Bodas, and V. Gajbhiye, *Nanomedicine* **13**, 1221 (2018).
- [5] K. Wu, D. Su, J. Liu, R. Saha, and J.-P. Wang, *Nanotechnology* **30**, 502003 (2019).
- [6] A. Rivera-Rodriguez and C. M. Rinaldi-Ramos, *Annu. Rev. Chem. Biomol. Eng.* **12**, 163 (2021).
- [7] W. T. Coffey, Yu. P. Kalmykov, and S. V. Titov, *Thermal Fluctuations and Relaxation Processes in Nanomagnets* (World Scientific, Singapore, 2020).
- [8] V. I. Stepanov and M. Shliomis, *Bull. Russ. Acad. Sci. Phys.* **55**, 1042 (1991).
- [9] R. Taululis and A. Cēbers, *Phys. Rev. E* **86**, 061405 (2012).
- [10] P. Ilg, *Phys. Rev. E* **100**, 022608 (2019).
- [11] Yu. L. Raikher and V. I. Stepanov, *Adv. Chem. Phys.* **129**, 419 (2004).
- [12] Yu. L. Raikher and V. I. Stepanov, *J. Magn. Magn. Mater.* **368**, 421 (2014).
- [13] I. S. Poperechny, *J. Mol. Liq.* **299**, 112109 (2020).
- [14] J. Weizenecker, *Phys. Med. Biol.* **63**, 035004 (2018).
- [15] S. V. Titov, W. T. Coffey, Yu. P. Kalmykov, M. Zarifakis, and A. S. Titov, *Phys. Rev. E* **103**, 052128 (2021).
- [16] P. Ilg and M. Kröger, *Phys. Rev. B* **106**, 134433 (2022).
- [17] D. A. Varshalovich, A. N. Moskalev, and V. K. Khersonsky, *Quantum Theory of Angular Momentum: Irreducible Tensors, Spherical Harmonics, Vector Coupling Coefficients, 3nj Symbols* (World Scientific, Singapore, 1988).
- [18] W. T. Coffey, P. J. Cregg, D. S. F. Crothers, J. T. Waldron, and A. W. Wickstead (2019).
- [19] I. S. Poperechny, Yu. L. Raikher, and V. I. Stepanov, *Phys. Rev. B* **82**, 174423 (2010).
- [20] Yu. L. Raikher and V. I. Stepanov, *Phys. Rev. B* **50**, 6250 (1994).
- [21] I. S. Poperechny, Yu. L. Raikher, and V. I. Stepanov, *J. Magn. Magn. Mater.* **424**, 185 (2017).
- [22] B. A. Storonkin, *Sov. Phys. Cryst.* **30**, 489 (1985).
- [23] W. T. Coffey, Yu. P. Kalmykov, and J. T. Waldron, *The Langevin Equation*, 4th ed. (World Scientific, Singapore, 2017).
- [24] W. F. Brown, *IEEE Trans. Magn.* **15**, 1196 (1979).
- [25] Yu. P. Kalmykov, *J. Appl. Phys.* **96**, 1138 (2004).
- [26] Yu. L. Raikher and M. I. Shliomis, *Adv. Chem. Phys.* **87**, 595 (1994).
- [27] T. Yoshida and K. Enpuku, *Jpn. J. Appl. Phys.* **48**, 127002 (2009).
- [28] J. Dieckhoff, D. Eberbeck, M. Schilling, and F. Ludwig, *J. Appl. Phys.* **119**, 043903 (2016).